Pergamon

Tetrahedron 55 (1999) 5027–5046

TETRAHEDRON

Photochemical Studies on the Through-space S···S Interaction of 2-Phenylnaphtho[1,8-*de*][1,3]dithiin 1-Oxide, 5-Phenyl[1]benzothieno[4,3,2-*def*][1,3]benzodithiepin 4-Oxide, and 2-Phenyldibenzo[*d,f*][1,3]dithiepin 1-Oxide

Takayoshi Fujii,*[,†,‡] Hiroki Kusanagi,[†] Ohgi Takahashi,[†]
Ernst Horn,[†,§] Naomichi Furukawa*[,†]

† *Tsukuba Advanced Research Alliance Center and Department of Chemistry, University of Tsukuba, Tsukuba, Ibaraki 305-8571, Japan*
‡ *Department of System Engineering of Materials and Life Science, Faculty of Engineering, Toyama University, Gofuku, Toyama 930-8555, Japan*
§ *Department of Chemistry, Rikkyo University, Nishi-Ikebukuro, Tokyo 171-8501, Japan*

Received 13 November 1998; accepted 1 March 1999

Abstract: 2-Phenylnaphtho[1,8-*de*][1,3]dithiin 1-oxide (**4a**), 5-phenyl[1]benzothieno[4,3,2-*def*][1,3]-benzodithiepin 4-oxide (**4b**), and 2-phenyldibenzo[*d,f*][1,3]dithiepin 1-oxide (**4c**) underwent facile consecutive photochemical reactions to give the corresponding disulfide, naphtho[1,8-*cd*][1,2]dithiole (**1a**), [1]benzothieno[4,3,2-*cde*][1,2]benzodithiin (**1b**), and dibenzo[*c,e*][1,2]dithiin (**1c**) and benzaldehyde (**7**), respectively, *via* the sulfur-sulfur (S···S) interaction. The proposed mechanism for these photochemical reactions is based on the quantum yields measurements, photo-intensity effects, and sensitizer effects. *Ab initio* calculations were also carried out for a model compound of the primary photoproduct, which showed that the S···S distance becomes shorter and the S–O distance becomes longer upon the excitation to the S_1 state.

Introduction

Transannular interactions or through-space interactions have often been observed between two or more heteroatoms that are arranged appropriately in one molecule.[1-8] Especially, the interactions between the sulfur atoms are of interest in determining the geometry of molecules, their reactivity, and their biological properties. There are numerous examples of such transannular interactions in the sulfur and selenium compounds. For example, the diagnosis of the proximity effects between the two sulfur and selenium atoms in 1,8-dichalcogen-substituted naphthalenes and 1,9-dichalcogen-substituted dibenzochalcogenophenes is indicated by their unusually low oxidation potentials as compared with normal mono-sulfides and –selenides.[3,4i,5a-c] When these sulfur or selenium compounds and the corresponding monooxides were treated with strong acids or acid anhydrides such as concentrated sulfuric acid or trifluoromethanesulfonic anhydride [$(CF_3SO_2)_2O$], they gave the corresponding dithia- and diselena- dications *via* probably the initial formation of cation radicals, and the dithia- or diselena- dications were treated with water to give the corresponding sulfoxides or selenoxides again in high yields.[3,4f-i,5a-c]

0040-4020/99/$ - see front matter
PII: S0040-4020(99)00201-X

In the course of our studies with respect to the through-space interaction of 1,8-disubstituted naphthalenes and 1,9-disubstituted dibenzochalcogenophenes, we have succeeded in generating reactive species such as *o*-quinodimethane[6] on photolysis of 8,13-dihydrobenzo[*g*]naphtho[1,8-*bc*][1,5]diselenonin and releasing carbonyl compounds[7a], *N*-tosylaldimines[7b,c], and olefins[7e] on photolysis of naphtho[1,8-*de*][1,3]-dithiin-1-oxides, -1-*N*-tosylsulfilimines, and -1-bis(ethoxycarbonyl)methylides. Photodecomposition of [1]benzothieno[4,3,2-*def*][1,3]benzodithiepin 4-oxides also provided quantitatively the corresponding carbonyl compounds.[5f] Furthermore, we have succeeded in the first preparation of dibenzo[*bn,fg*][1,4]dithiapentalene and its selenium analogs by thermolysis or photolysis of 1,9-disubstituted dibenzochalcogenophenes.[5d] We suggested that the photodecomposition of these compounds proceeded by the interaction between the two sulfur or selenium atoms at the 1,8-positions of naphthalene and 1,9-positions of dibenzochalcogenophene. Quite recently, we carried out an *ab initio* calculation of an excited state (S_1) of naphtho[1,8-*ef*][1,4]dithiepin as a model compound.[7f] The result showed that the excitation to the S_1 state causes the S···S bonding interaction, and this is related to the clean photodecomposition of naphtho[1,8-*ef*][1,4]dithiepins to olefins. In order to examine the potential of the sulfur-sulfur interaction during the photoreaction, we studied the photolysis of 2-phenylnaphtho[1,8-*de*][1,3]dithiin 1-oxide (**4a**), 5-phenyl[1]benzothieno[4,3,2-*def*][1,3]benzodithiepin 4-oxide (**4b**), and 2-phenyldibenzo[*d,f*][1,3]dithiepin 1-oxide (**4c**) and also carried out *ab initio* calculations for a model compound of the primary photoproducts in the present photolysis.

Results

Synthesis. 2-Phenylnaphtho[1,8-*de*][1,3]dithiin 1-oxide (**4a** and **4a'**) was prepared according to the following procedures (Scheme 1). Naphtho[1,8-*cd*][1,2]dithiole (**1a**) was prepared according to the method reported in the literature.[9,10] Reduction of **1a** with sodium borohydride in THF-ethanol at room temperature almost quantitatively gave 1,8-naphthalenedithiol (**2a**).[11] Compound **2a** was treated with benzaldehyde (**7**) in the presence of $SiCl_4$ in CH_2Cl_2 affording the corresponding 2-phenylnaphtho[1,8-*de*][1,3]dithiin (**3a**) in 98% yield.[12] Compounds **4a** and **4a'** were obtained in a total yield of 96% as a mixture of diastereoisomers (**4a** : **4a'** = 5 : 1) by oxidation of **3a** using *m*-chloroperbenzoic acid (*m*CPBA) in CH_2Cl_2 at -20 °C. 5-phenyl[1]benzothieno[4,3,2-*def*][1,3]benzodithiepin 4-oxide (**4b**) was prepared from [1]benzothieno[4,3,2-*cde*][1,2]benzodithiin (**1b**) (Scheme 2). 1,9-Bis(methylthio)dibenzothiophene[13] was treated initially with sodium methylthiolate in DMF at reflux conditions, and subsequently with iodine at room temperature to give **1b** in 92 % yield.[14] Compound **1b** was reduced with sodium borohydride to 1,9-dibenzothiophenedithiol (**2b**), which was subsequently treated with **7** in the presence of $SiCl_4$ in CH_2Cl_2 at - 20 °C to give 5-phenyl[1]benzothieno[4,3,2-*def*][1,3]benzodithiepin (**3b**) in 79% yield. Compounds **4b** and **4b'** were obtained in a total yield of 84% as a mixture of diastereoisomers (**4b** : **4b'** = 2 : 1) by oxidation of **3b** using *m*-chloroperbenzoic acid (*m*CPBA) in CH_2Cl_2 at -20 °C. 2-Phenyldibenzo[*d,f*][1,3]dithiepin (**3c**) was prepared by a method similar to the synthesis of **3a** using dibenzo[*c,e*][1,2]dithiin (**1c**). 2-Phenyldibenzo[*d,f*][1,3]di-

thiepin 1-oxide (**4c** and **4c'**) was obtained in a 90% yield with high diastereo-selectivity (**4c** : **4c'** = 10 : 1) by oxidation of **3c** using *m*CPBA in CH_2Cl_2 at -20 °C (Scheme 3).

Scheme 1

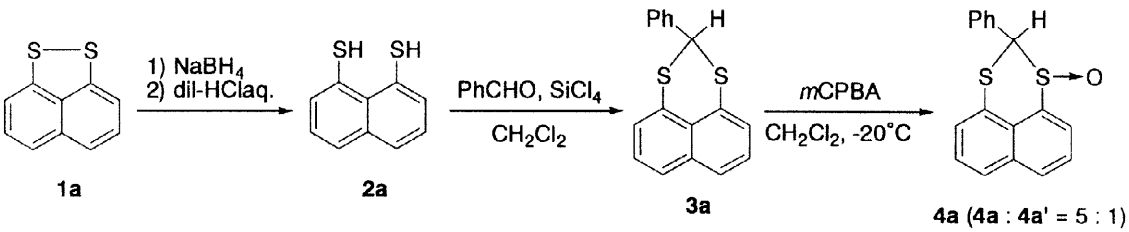

1a 2a 3a 4a (4a : 4a' = 5 : 1)

Scheme 2

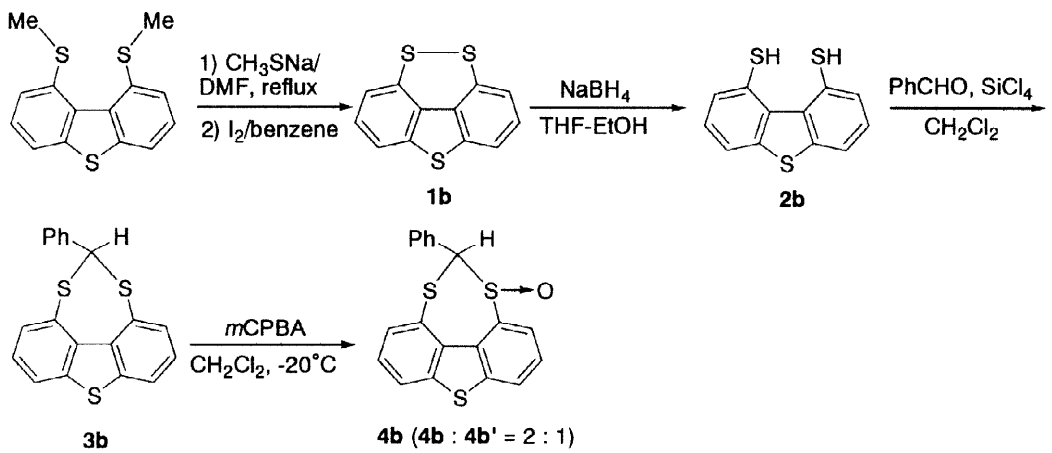

1b 2b 3b 4b (4b : 4b' = 2 : 1)

Scheme 3

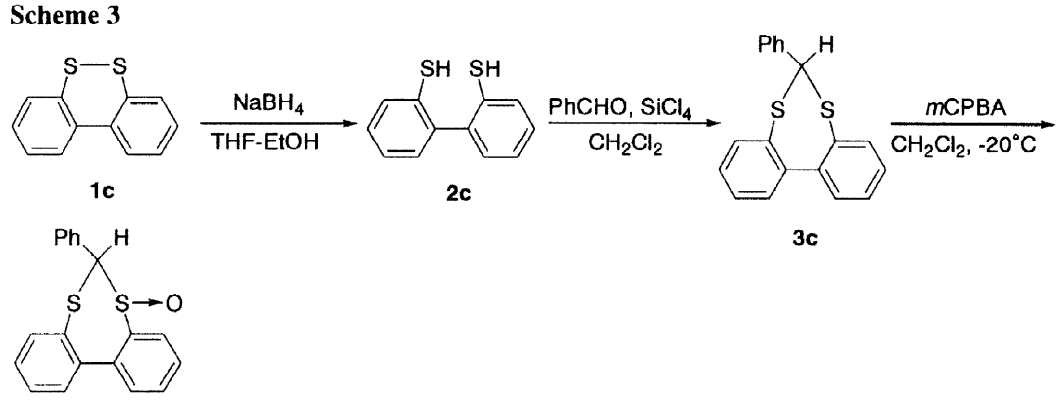

1c 2c 3c 4c (4c : 4c' = 10 : 1)

X-ray Crystallographic Analysis. The detailed structural analysis of the major diasteroisomers 5-phenyl[1]benzothieno[4,3,2-*def*][1,3]benzodithiepin 4-oxide (**4b**) and 2-phenyldibenzo[*d,f*][1,3]dithiepin 1-oxide (**4c**) was performed by X-ray crystallographic analysis (Figures 1 and 2). The molecular structure of **4b** is a *trans*-isomer with a phenyl group and a sulfinyl-oxygen atom occupying the equatorial positions (R_S, S_C and S_S, R_C configurations), and hence the other structure **4b'** should be a racemic mixture of S_S, S_C and R_S, R_C

configurations. The torsional angle (C(1)-C(12)-C(11)-C(10)) of **4b** is 4.5° revealing that the central dibenzothiophene ring is nearly a planar skeleton as compared with the corresponding angle of 1-(phenylsulfenyl)-9-(phenylsulfinyl)-dibenzothiophene (19.1°).[5e] The S(1)···S(2) distance of **4b** is 2.89 Å, which is markedly shorter than the sum of the van der Waals radii (3.70 Å) of sulfur atoms.

4c also has a *trans*-isomeric structure with a phenyl group and a sulfinyl-oxygen atom occupying the equatorial positions (R_S, S_C and S_S, R_C configurations; thus, the configurations of **4c'** should be S_S, S_C and R_S, R_C). The torsional angle (C(1)-C(6)-C(7)-C(16)) of **4c** is 53.0°, which indicates a considerably twisted structure due to lone pair–lone pair repulsion between the sulfur atoms attached at the 1,1'-positions of biphenyl ring. Therefore, the S(1)···S(2) distance of **4c** is 3.08 Å, which is about 0.2 Å longer than that of **4b**.

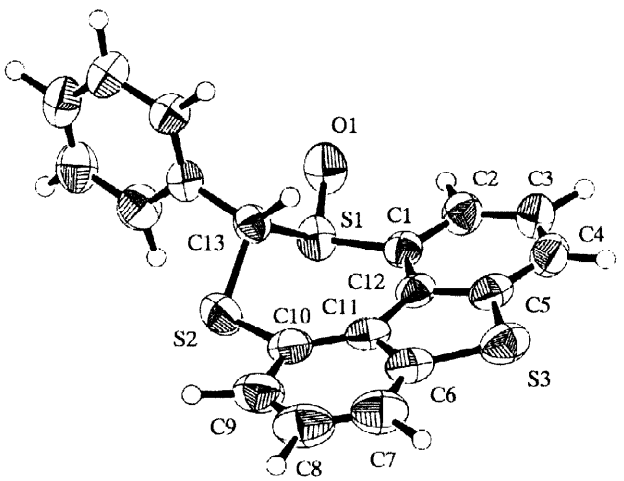

Figure 1. ORTEP Drawing of **4b**

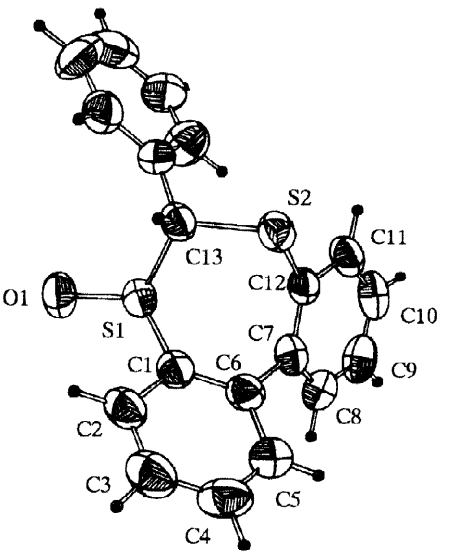

Figure 2. ORTEP Drawing of **4c**

Photolysis. Preparative scale photoreactions of 2-phenylnaphtho[1,8-*de*][1,3]dithiin 1-oxide (**4a**), 5-phenyl[1]benzothieno[4,3,2-*def*][1,3]benzodithiepin 4-oxide (**4b**), and 2-phenyldibenzo[*d,f*][1,3]dithiepin 1-oxide (**4c**) in deoxygenated CH_2Cl_2 were carried out in a Pyrex round-bottomed flask using a high pressure mercury lamp (500 W, > 300 nm) at room temperature (Scheme 4, See Experimental Section). The photoreactions of **4a** and **4b** were completed within 6 h, giving the corresponding disulfide, naphtho[1,8-*cd*][1,2]dithiole (**1a**) and [1]benzothieno[4,3,2-*cde*][1,2]benzodithiin (**1b**), and benzaldehyde (**7**) quantitatively. However, **4c** decomposed slowly (3 days) to give dibenzo[*c,e*][1,2]dithiin (**1c**), **7**, and a small amount of dibenzo[*ce*][1,2]dithiin 1-oxide. Since the formation of dibenzo[*ce*][1,2]dithiin 1-oxide was observed at longer irradiation time, this compound may be formed by photooxidation. Solvent effects were examined on photolysis of **4a-c** using protic and aprotic solvents including ethanol, acetonitrile, THF, and benzene. The photodecomposition reactions gave **1a-c** and **7** almost quantitatively regardless of the solvent used. The

consumption of **4a-c** and the formation of products **1a-c** and **7** were unaffected by the addition of benzophenone as a triplet sensitizer and isoprene as a triplet quencher, indicating that the reaction may proceed *via* an excited singlet state, perhaps the lowest excited singlet (S_1) state.

The reaction profile for the photoreaction of **4a** in $CDCl_3$ under irradiation with a high pressure mercury lamp (500 W, λ = 313 nm) is shown in Figure 3. The HPLC profiles in CH_2Cl_2 were also similar to that of ^{1}H-NMR conditions. The ^{1}H -NMR peak of the starting material **4a** at δ 4.92 (s, 1H, CH) gradually reduced, while the peak of the photo-rearranged intermediate, 3-hydro-3-phenylnaphtho[1,8-*ef*][1,4]dithia[2]oxepine (**6a**) (δ 6.73 (s, CH)), together with that of the products **1a** (δ 7.14 (d, J = 7.6 Hz, Naph-H)), **7** (δ 10.03 (s, CHO)) and the photo-isomerized compound **4a'** (5.35 (s, CH)) increased. The products **1a**, **4a'**, and **7** were identified by comparing the spectral data of the authentically prepared compounds. The ^{1}H-NMR signals of the intermediate **6a** increased gradually but disappeared soon and the spectra changed to those of the products **1a** and **7**. When the photolysis of **4a** was stopped at the optimum point of conversion of **4a** to **6a**, the intermediate **6a** could be obtained in 95% purity by preparative HPLC from the reaction mixture. The intermediate **6a** is an unstable, acid-sensitive and oily material and its ^{1}H-, ^{13}C-NMR, and mass spectral data are consistent with the structure shown in Scheme 4. The photolysis of **6a** provided **1a** and **7**.

Photolysis of **4b** under irradiation with a high pressure mercury lamp (500 W, λ = 313 nm) in deoxygenated CH_2Cl_2 was monitored by HPLC at various time intervals (Figure 4). The progress of the reaction in $CDCl_3$ was also followed by ^{1}H-NMR spectroscopy and gave similar results. Attempts to detect the intermediate generated from this reaction by HPLC and ^{1}H-NMR conditions failed. However, when the photolysis of **4b** was stopped at the optimum point of conversion of **4b** to **6b** which is estimated from the mass balance (Figure 4), the intermediate **6b** could be obtained with 89% purity by preparative HPLC of the reaction mixture and its structure was determined by ^{1}H-NMR ($CDCl_3$, 55 °C) and mass spectral data (see Scheme 4). The intermediate **6b** is also an unstable, acid-sensitive and oily material. The ^{1}H-NMR spectra of **6b** at room temperature showed broad aromatic protons but a methyne proton was not observed. Therefore, it is difficult to detect the intermediate by ^{1}H-NMR at the present conditions. The crude **6b** also underwent photodecomposition giving **1b** and **7** under the photochemical conditions above described. The apparent mass balance dipped and rose again in a manner completely consistent with the formation of the intermediate **6b**. The quantitative mass balance observed in the present photolysis was achieved reproducibly on extended photolysis.

The progress for the photolysis of **4c** in CH_2Cl_2 under similar photolysis conditions was followed at room temperature by HPLC (Figure 5). Photolysis was stopped after 16 h. The starting material **4c** reduced gradually to give the isomerized compounds **4c'**, **7**, and dibenzo[*c*,*e*][1,2]dithiole (**1c**). The products **1c**, **4c'**, and **7** were identified by comparing their retention times with those of the authentic compounds. The peak of **4c'** increased gradually and its maximum was reached at approximately 46% of the reaction mixture. This

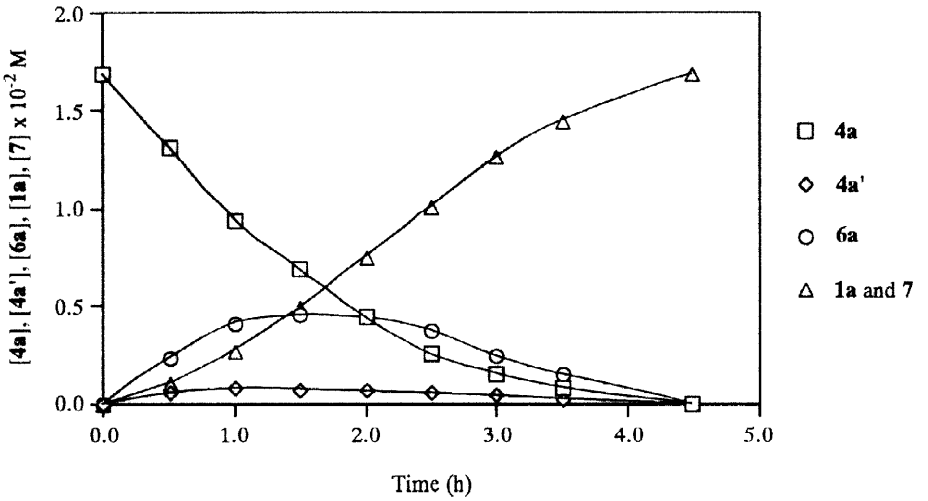

Figure 3. Time course of photolysis of **4a** (1.69×10^{-2} M **4a** in $CDCl_3$).

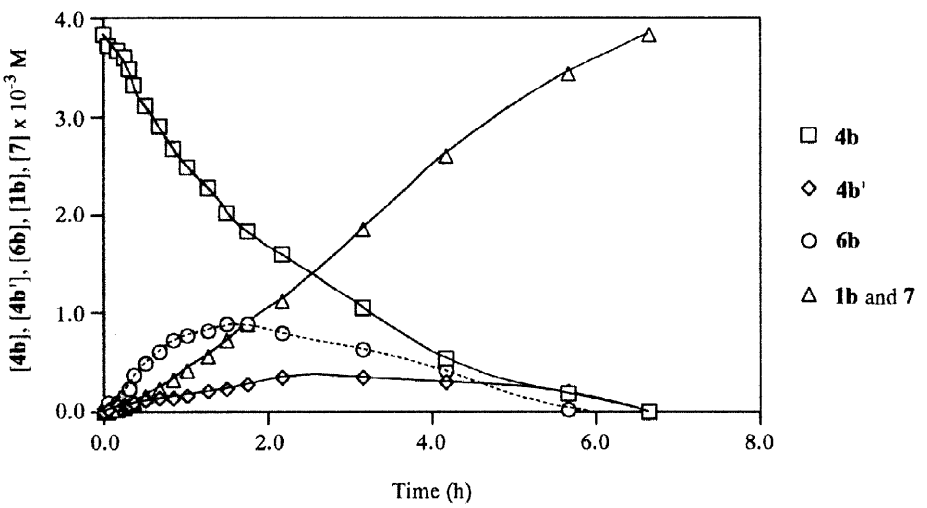

Figure 4. Time course of photolysis of **4b** (3.84×10^{-3} M **4b** in CH_2Cl_2).

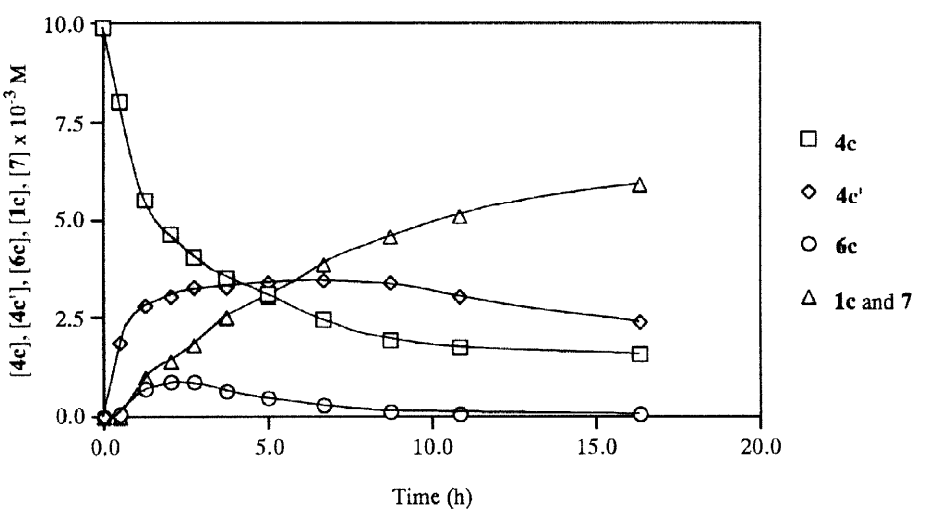

Figure 5. Time course of photolysis of **4c** (9.94×10^{-3} M **4c** in $CDCl_3$).

time course experiment has also been done by ^{1}H-NMR conditions. During this reaction, a weak absorption peak started to appear at 5.91 ppm, which is assigned to the signal due to the intermediate **6c** (see Scheme 4), in addition to the peaks due to **4c** (δ 4.97, s, CH), **4c'** (δ 6.09, s, CH), **7**, (δ 10.03, s, 1H, CHO), and **1c** (δ 7.70, d, ArH). This peak reached an approximate maximum of 9% of the reaction mixture as determined by the relative peak integrals of the reaction mixture in the ^{1}H-NMR spectrum, and then almost disappeared and the spectra were converted to those of the products **1c** and **7**. This intermediate **6c** was amenable to detection only by ^{1}H-NMR spectroscopy, and we could not isolate it from the reaction mixture.

Light Intensity Effects. The effect of light intensity on photolysis of sulfoxides **4a-c** was studied in order to understand whether the reaction proceeds by a one-, two- or multi-photon process. In the case of 2-phenylnaphtho[1,8-*de*][1,3]dithiin 1-oxide (**4a**), the loss of **4a** was proportional to the first power of the intensity of 313 nm light, whereas the formation of **1a** and **7** was proportional to the square of the intensity as shown in Figure 6. These results imply that the consumption of **4a** proceeds by a one-photon process to give an intermediate **6a** in the primary photochemical step. Thereafter, the intermediate **6a** should be converted to **1a** and **7** in the secondary photochemical step. The effect of light intensity on photolysis of 5-phenyl[1]benzothieno[4,3,2-*def*][1,3]benzodithiepin 4-oxide (**4b**) also gave results similar to those obtained for **4a** (Figure 7). Thus, in the primary photochemical step an intermediate **6b** may be formed by a one-photon process and be followed to give **1b** and **7** *via* a one-photon process. On the other hand, the loss of 2-phenyldibenzo[*d,f*][1,3]dithiepin 1-oxide (**4c**) and the formation of **1c** and **7** were not proportional to either first or square with respect to the intensity. As can be seen from Figure 5, this result is due to the isomerized reaction during the photon process. Since up to 35 %, the loss of **1b** was proportional to the first power of the intensity, this reaction may also proceed *via* a manner similar to the photoreactions of **4a** and **4b**.

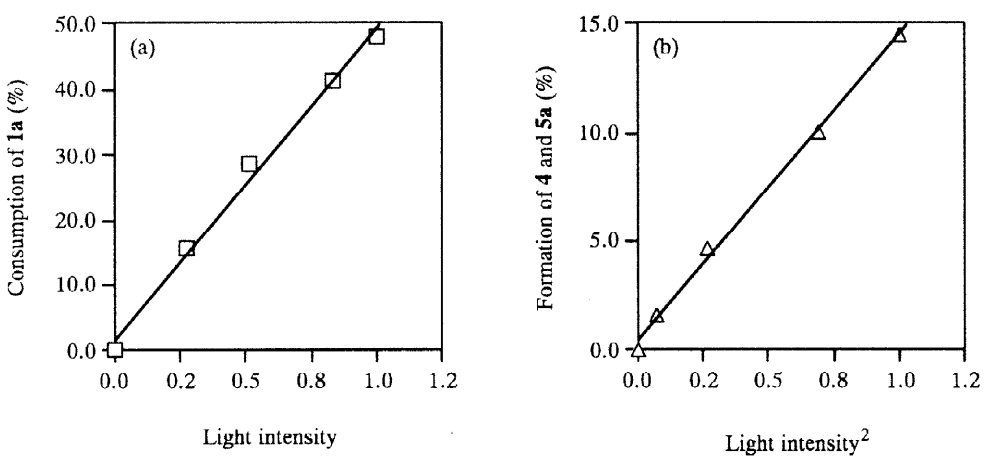

Figure 6. Light intensity dependence on the consumption of **4a** (a) and the formation of **1a** and **7** (b) (4.87×10^{-3} M **4a** in CH_2Cl_2).

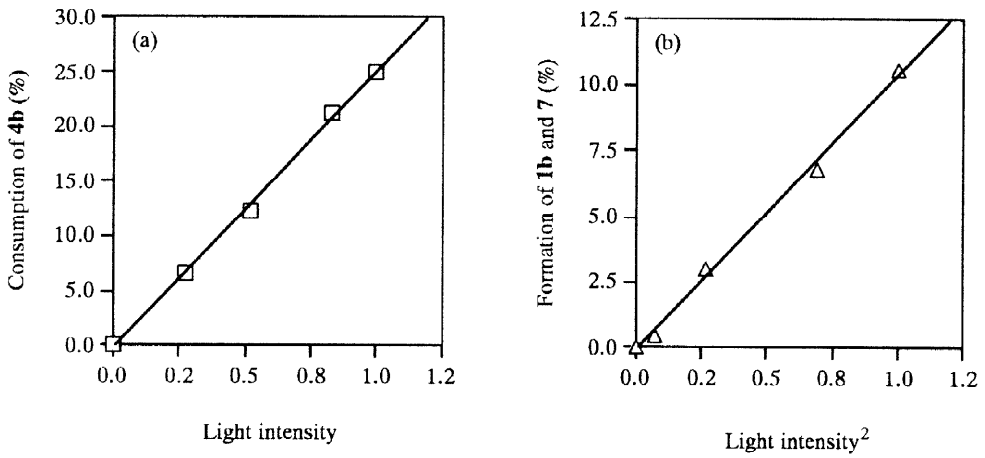

Figure 7. Light intensity dependence on the consumption of **4b** (a) and the formation of **1b** and **7** (b) (4.02×10^{-3} M **4b** in CH_2Cl_2).

Quantum Yield. The formation of isolable products such as disulfides **1** and benzaldehyde (**7**) was revealed to proceed *via* a two photon event. Therefore, the meaningful quantum yields are those for the loss of starting materials **4** and the formation of isomerized product **4'** and sulfenic esters **6** as an intermediate. However, the intermediates **6a** and **6b** were unstable and **6c** could not be isolated. Therefore, the intermediates **6** could not be analyzed by HPLC conditions. The quantum yields for the consumption of substrates (**4** or **4'**) ($\Phi_{consumed}$) and the formation of the isomerized compounds (**4'** and **4**) ($\Phi_{inv.}$) using a high pressure mercury lamp (500 W, 313 nm) at room temperature in deoxygenated CH_2Cl_2 were measured by comparison with fulgide actinometry[15] as shown in Table 1.

Table 1. Quantum Yield for Consumption of **4a-c** and **4a'-c'**[a)]

4	Φ_{loss} [b)]	$\Phi_{inv.}$ [b)]	$\Phi_{loss}/\Phi_{cleave}$ [c)]	$\Phi_{inv.}/\Phi_{cleave}$ [c)]
a	0.27	0.020	0.87	0.06
a'	0.62	0.070	0.82	0.09
b	0.29	0.050	0.74	0.13
b'	0.33	0.056	0.74	0.13
c	0.10	0.040	0.55	0.22
c'	0.17	0.061	0.58	0.21

a) Light was provided by a 500 W high pressure Hg lamp filtered throug a Toshiba UVD33s and a monochromator set at 313 nm. b) Fulgide was the actinometer. $\Phi_{loss} = \Phi_{consumed} - \Phi_{inv.}$ c) $\Phi_{cleave} = \Phi_{loss} + 2\Phi_{inv.}$

***Ab initio* Calculation of 3-Hydro-3-phenylnaphtho[1,8-*ef*][1,4]dithia[2]oxepine (6a).** In order to gain insight into the mechanism of the second step of the present photolysis reactions of **4**, i.e. the photodecomposition of the primary photoproducts **6**, *ab initio* calculations were performed for the S_0 and S_1 states of the model compound **8**. Another purpose of the calculations was to compare the results with those for the carbon analogue **9** reported previously.[7f] Calculations were performed using SPARTAN[16] and GAUSSIAN 92[17].

Table 2 Optimized Geometries for the S_0 and S_1 states of **8**[a)]

Parameters	S_0 (STO-3G*)	S_0 (3-21G(*))	S_0 (6-31G*)	S_1 (STO-3G*)	S_1 (3-21G(*))
Interatomic Distances (Å)					
S(1)–C(1)	1.763	1.772	1.776	1.725	1.731
S(1)–O(1)	1.627	1.647	1.649	1.882	2.091
S(2)–C(9)	1.761	1.784	1.787	1.751	1.773
S(2)–C(11)	1.778	1.796	1.805	1.838	1.871
C(1)–C(2)	1.365	1.364	1.365	1.376	1.373
C(1)–C(10)	1.451	1.438	1.439	1.444	1.436
C(2)–C(3)	1.419	1.406	1.409	1.414	1.402
C(3)–C(4)	1.351	1.351	1.353	1.359	1.356
C(4)–C(5)	1.431	1.418	1.420	1.427	1.416
C(5)–C(6)	1.432	1.417	1.420	1.433	1.415
C(5)–C(10)	1.410	1.418	1.417	1.404	1.415
C(6)–C(7)	1.350	1.351	1.352	1.353	1.354
C(7)–C(8)	1.420	1.407	1.411	1.424	1.405
C(8)–C(9)	1.365	1.364	1.364	1.362	1.366
C(9)–C(10)	1.453	1.439	1.441	1.440	1.430
O(1)–C(11)	1.456	1.456	1.403	1.413	1.382
S(1)···S(2)	2.959	3.067	3.102	2.540	2.937
Interatomic Angles (deg)					
C(1)–S(1)–O(1)	101.1	101.8	100.2	93.9	87.5
C(9)–S(2)–C(11)	100.9	102.0	103.4	100.4	98.5
S(1)–C(1)–C(2)	116.6	114.9	114.5	120.1	115.6
S(1)–C(1)–C(10)	124.0	124.9	124.9	121.1	124.2
C(2)–C(1)–C(10)	119.4	120.1	120.5	118.7	120.2
C(1)–C(2)–C(3)	122.0	122.1	121.8	121.0	121.6
C(2)–C(3)–C(4)	119.6	119.3	119.2	120.9	119.5
C(3)–C(4)–C(5)	120.8	120.9	121.0	120.2	121.0
C(4)–C(5)–C(6)	119.6	118.9	118.8	121.9	119.4
C(4)–C(5)–C(10)	120.2	120.5	120.6	119.3	120.4
C(6)–C(5)–C(10)	120.2	120.6	120.6	118.8	120.2
C(5)–C(6)–C(7)	120.8	120.9	120.9	120.9	120.7
C(6)–C(7)–C(8)	119.5	119.3	119.3	120.3	119.5
C(7)–C(8)–C(9)	122.1	122.0	122.0	120.8	121.9
S(2)–C(9)–C(8)	116.2	115.0	115.0	120.9	116.9
S(2)–C(9)–C(10)	124.1	124.5	124.3	119.4	123.2
C(8)–C(9)–C(10)	119.4	120.2	120.2	119.7	119.8
C(1)–C(10)–C(5)	117.9	117.0	116.7	119.8	117.2
C(1)–C(10)–C(9)	124.1	126.1	126.3	120.6	124.9
C(5)–C(10)–C(9)	117.9	116.9	117.0	119.6	117.8
S(1)–O(1)–C(11)	115.5	120.2	118.3	105.0	108.7
S(2)–C(11)–O(1)	115.4	114.3	114.7	110.0	108.9
Dihedral Angles (deg)					
S(1)–C(1)–C(10)–C(9)	2.3	0.3	2.8	–3.2	9.3
C(1)–C(10)–C(9)–S(2)	8.1	10.0	14.4	0.1	1.1
C(10)–C(9)–S(2)–C(11)	–67.6	–67.0	–68.0	–69.6	–72.8
C(9)–S(2)–C(11)–O(1)	66.1	63.9	50.3	80.8	52.6
S(1)–O(1)–C(11)–S(2)	17.6	17.5	37.0	7.2	38.3
C(1)–S(1)–O(1)–C(11)	–88.1	–84.8	–95.2	–92.9	–109.1
O(1)–S(1)–C(1)–C(10)	57.8	54.9	48.5	76.0	51.8
C(2)–C(1)–C(10)–C(9)	–176.4	–178.9	–178.0	–179.4	–172.1
C(10)–C(1)–C(2)–C(3)	–0.9	0.9	0.8	–0.6	–5.0
C(1)–C(2)–C(3)–C(4)	–1.6	–2.9	–3.7	1.1	2.1
C(2)–C(3)–C(4)–C(5)	2.0	1.7	2.4	–0.4	1.5
C(3)–C(4)–C(5)–C(6)	178.8	–178.9	–178.6	178.8	176.4
C(4)–C(5)–C(6)–C(7)	–177.8	–179.5	–179.3	–179.2	–176.7
C(5)–C(6)–C(7)–C(8)	0.5	1.2	1.8	–0.7	0.3
C(6)–C(7)–C(8)–C(9)	–1.0	–0.4	–1.0	0.0	–1.6
C(7)–C(8)–C(9)–C(10)	0.0	–1.6	–1.8	0.9	0.6
C(8)–C(9)–C(10)–C(1)	–179.3	–176.3	–174.9	177.7	177.8
C(1)–C(10)–C(5)–C(4)	–2.5	–3.3	–4.7	1.3	–0.8
C(9)–C(10)–C(5)–C(4)	176.8	177.6	176.6	180.0	175.8

a) The atom-labeling scheme is shown in Figure 8.

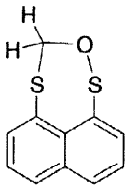

8

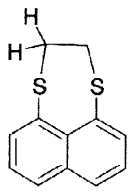

9

Ab initio calculations for the S_0 state of **8** were performed at the RHF level with the STO-3G*, 3-21G(*), and 6-31G* basis sets. Selected structural parameters of the optimized geometries are shown in Table 2. Figure 8 shows a three-dimensional view of the 3-21G(*) structure. At the geometries optimized for S_0 with STO-3G* and 3-21G(*), the S_1 state was calculated by CIS/STO-3G* and CIS/3-21G(*) methods, respectively. The largest component in the S_1 wave functions was the HOMO→LUMO excitation (34 and 33%, respectively). Geometry optimizations for the S_1 state were carried out by both the CIS/STO-3G* and CIS/3-21G(*) methods. The results are also included in Table 2. Figure 8 shows both geometries ((b) and (c)).

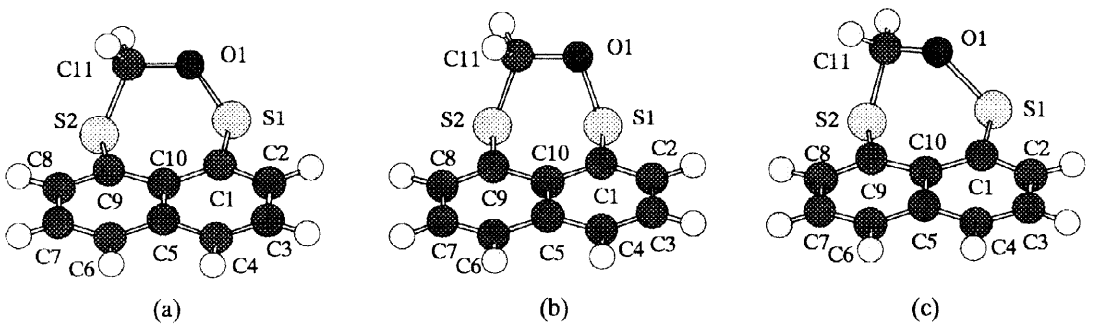

Figure 8. Three-dimensional view for the RHF/3-21G(*) optimized S0 structure (a) and the S1 structures optimized by CIS/STO-3G* (b) and CIS/3-21G(*) (c) of **8**.

Discussion

These results show that photolysis of 2-phenylnaphtho[1,8-*de*][1,3]dithiin 1-oxide (**4a**), 5-phenyl[1]benzothieno[4,3,2-*def*][1,3]benzodithiepin 4-oxide (**4b**) and 6-phenyldibenzo[*d,f*][1,3]dithiepin 1-oxide (**4c**) using a high pressure mercury lamp proceeds as follows: (1) The primary process was that the photolysis of sulfoxides **4** and **4'** gave the corresponding racemized sulfoxides and sulfenic esters **6**, respectively, in an excited singlet state in a one photon process. (2) The sulfenic esters **6** underwent photodecomposition giving the corresponding disulfides **1** and benzaldehyde (**7**), respectively, in the secondary photochemical step. It is well known that many photochemical reactions of sulfoxides proceed *via* an initial formation of sulfenic esters as intermediates.[18] Several sulfenic esters were isolated after photolysis of acyclic[18c] and cyclic sulfoxides.[18b,19] Photolysis of sulfenic esters proceeds through S-O bond cleavage to yield sulfinyl and alkoxyl radicals which afford thiol, aldehyde, and others by disproportionation.[18c,20]

This photo-rearrangement of **4** to sulfenic ester **6** may be caused by a through-space interaction between the two sulfur atoms in the ground or excited state. The X-ray analysis clearly reveals that the S(1)···S(2) distances in the sulfoxides **4b** and **4c** are 2.89 and 3.07 Å, respectively, and are markedly shorter than the sum of the van der Waals radii of two sulfur atoms (3.70 Å). Single crystals of 2-phenylnaphtho[1,8-*de*][1,3]dithiin 1-oxide could not be obtained. According to our previous results, the S···S distance of the isoelectronic 2-methylnaphtho[1,8-*de*][1,3]dithiin 1-*N*-tosylsulfilimine is 2.86 Å, which is shorter than that of 2,2-dihydronaphtho[1,8-*de*][1,3]dithiin (2.96 Å).[7c] Glass and co-workers have reported that the S···S distance of 3.00 Å for naphthalene[1,8-*b,c*][1,5]dithiocin 1-oxide is about 0.2 Å shorter than that of the corresponding dithioether (3.23 Å)[4h], and hence we expect that the S···S distance of **4a** is shorter than that of 2,2-dihydronaphtho[1,8-*de*][1,3]dithiin (2.96 Å). These results imply that an attractive interaction between the two sulfur atoms in the 1,8-positions of the naphthalene, 1,9-positions of dibenzothiophene, and 2,2'-position of biphenyl exists in the sulfoxides **4**.

Recently, Jenks and Guo have received considerable attention for the photolysis of aryl benzyl sulfoxides.[18c] They concluded that the homolytic cleavage of sulfur-carbon bond on the photolysis of optically active benzyl *p*-tolyl sulfoxide was reversible with racemization by way of a cage recombination process. Racemization may result from the recombination of the geminated radical pair (RSO• and RCH_2•) which partitions between formation of the sulfenic ester and reversion to the starting material. They used the observed values of the quantum yield for the loss of benzyl *p*-tolyl sulfoxide (Φ_{loss}) and loss of optical activity ($\Phi_{rot.}$) to estimate the quantum yield of α-cleavage (eq.1).

$$\Phi_{inv.} = (\Phi_{rot.} - \Phi_{loss})/2$$
$$\Phi_{cleave} = \Phi_{loss} + 2\Phi_{inv.} = \Phi_{rot.}$$
eq. 1

Scheme 4

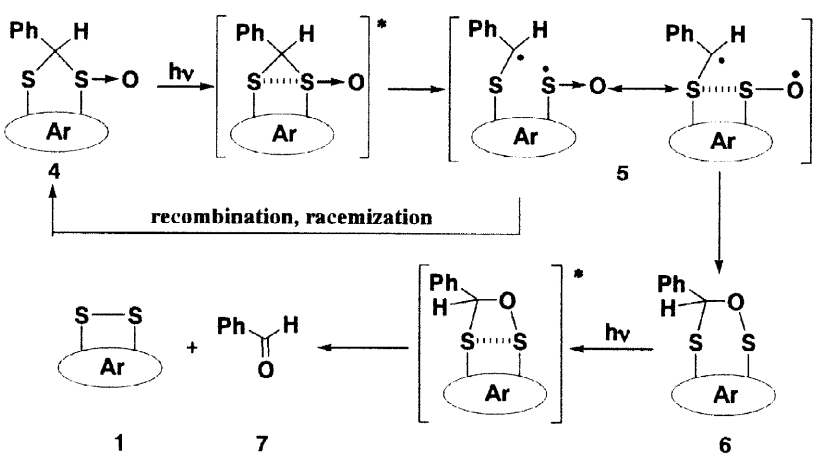

Ar = 1,8-Naphthalene (**4a**)
1,9-Dibenzothiophene (**4b**)
2,2'-Biphenyl (**4c**)

Our photoreaction may also be related to the above in Jenks and Guo's manner. For example, photolysis of **4** gave the corresponding **4'** and sulfenic ester **6**, respectively, in the primary photo step. In this case, sulfenic ester **6** plays no part in racemization, as photolysis of **6a** and **6b** does not yield **4a, a'** and **4b, b'**. If the excited states of sulfoxides **4** and **4'** were reversible with racemization by recombination of the biradical **5** or had a very low barrier for inversion, the through-space interactions between the two sulfur atoms at the 1,8-positions of naphthalene, 1,9-positions of dibenzothiophene, and 2,2'-positions of biphenyl play an important role particularly for the formation of sulfenic esters **6** on photolysis of sulfoxides (**4** and **4'**). As shown in Table 1, on the basis of the disappearance of the starting materials (**4** and **4'**) and their partial racemization, quantum yields of the cleavage (Φ_{cleave}) of sulfoxides **4a**, **4b**, and **4c** and their conversion (Φ_{loss}) to sulfenic esters **6a**, **6b**, and **6c** are estimated to be ≥0.31, ≥0.39, ≥0.18 and 0.27, 0.29, and 0.10, respectively. The estimated values of $\Phi_{loss}/\Phi_{cleave}$ for **4a** and **4b** are 0.87 and 0.74, which are larger than that for **4c** (0.55). The value of $\Phi_{loss}/\Phi_{cleave}$ for **4'** was also estimated to be very close to that for **4**. The results demonstrate that the photoreaction of 2-phenylnaphtho[1,8-*de*][1,3]dithiin 1-oxide (**4a**), 5-phenyl[1]benzothieno[4,3,2-*def*][1,3]benzodithiepin 4-oxide (**4b**), and 2-phenyldibenzo[*d,f*][1,3]dithiepane 1-oxide (**4c**) proceeds through the mechanism outlined in Scheme 4. An excited singlet state initiated cleavage of the carbon-sulfur bond in **4** gives the radical pair **5**. In the cases of **4a** and **4b**, the sulfinyl radical should be populated at the oxygen atoms, rather than at the sulfur atom *via* the strong attractive interaction between the two sulfur atoms to form the sulfenic esters **6a** and **6b** with recombination of RSO• and RSCH•. On the other hand, since the two sulfur atoms of **6c** can not be arranged appropriately to their participation due to rotating the C1-C1' bond in the biphenyl ring, sulfinyl radical of **6c** should be delocalized at the sulfur and oxygen atoms. This consideration explains that $\Phi_{loss}/\Phi_{cleave}$ of **4c** is 0.55, being indicative of approximately 1 : 1 formation of **4c'** and **4c**, which is very close to that of optically active benzyl *p*-tolyl sulfoxide (0.50)[18c].

In the secondary photochemical step, the intermediates **6** were converted to the corresponding disulfides **1** and benzaldehyde (**7**). This photochemical step proceeds *via* an excited singlet state as a one photon process. Since it was suggested that the photodecomposition of **6** proceeds *via* the S_1 state, we carried out *ab initio* calculations of model compound **8** in the S_1 state as well as in the ground state (S_0). In the optimized structures for the S_0 state of **8**, the naphthalene ring is appreciably twisted about the C(5)–C(10) axis, the exocyclic C–S bonds are splayed outward, and the sulfur atoms are displaced above and below the average plane of the naphthalene ring (in particular, the deviation of the S(2) atom from the plane is large). However, the extent of the deviation of the naphthalene ring and the sulfur atoms from planarity in **8** is somewhat smaller than those in **9**. The optimized S···S distances in the STO-3G*, 3-21G(*), and 6-31G* structures are 2.959, 3.067, and 3.102 Å, and are well within the van der Waals radius of sulfur (3.70 Å). Moreover, these distances are about 0.1 Å shorter than the corresponding distances of the carbon analogue **9** (3.060, 3.149, and 3.202 Å, respectively[7f]). This is due to a smaller size of an oxygen atom than a carbon

atom. However, the HOMO energies of **8**, –5.42 (STO-3G*), –7.84 (3-21G(*)), and –7.72 (6-31G*) eV, are lower than those of **9**[7f] (the HOMOs are an out-of-phase combination of the so-called σ*(S–S) orbital and the HOMO of naphthalene as in **9**). This is perhaps because the overlap between the two sulfur lone-pair orbitals is smaller due to their relative direction.

At the Franck–Condon geometry where the LUMO is essentially the LUMO of naphthalene, the HOMO→LUMO single excitation makes the largest contribution to the S_1 state. Since the HOMO is antibonding between the two sulfur atoms, it is expected that the relaxed S_1 geometry has an S···S distance which is shorter than that in the S_0 state. This was the case in both the STO-3G* and 3-21G(*) calculations, although the two methods gave considerably different results.

In the CIS/STO-3G* optimized S_1 structure, the S···S distance is 2.540 Å. Thus, the S···S distance becomes shorter by about 0.42 Å upon the excitation to S_1. Moreover, the S–O bond becomes longer by 0.255 Å, the S–C bond to be broken becomes longer by 0.06 Å, and the C–O bond becomes shorter by 0.043 Å on going from S_0 to S_1, while the bond lengths of the naphthalene ring do not change so much. These structural changes are one which is toward the products, **1a** and formaldehyde.

In the CIS/3-21G(*) optimized structure, the S···S distance is 2.937 Å, only 0.13 Å shorter than in the S_0 state. The S–O distance, however, is 2.091 Å, which is longer than in the S_0 state by 0.444 Å. The S–C bond is lengthened by 0.075 Å and the C–O bond shortens by 0.074 Å. Although the CIS/3-21G(*) structure is largely different from the CIS/STO-3G* structure, the trend in the structural change on going from S_0 to S_1 is similar in both basis sets.

At the CIS/STO-3G* geometry, the HOMO→(LUMO+1) excitation makes the largest (50%) contribution to the S_1 state, where the HOMO is essentially the σ*(S–S) orbital and the LUMO+1 is an in-phase combination of the σ*(S–O) and σ*(S–C) orbitals. At the CIS/3-21G(*) geometry, the HOMO→LUMO excitation is the largest (52%) component of the S_1 state, where the HOMO is σ*(S–S) – (naphthalene HOMO) and the LUMO is mainly composed of the σ*(S–O) orbital. The relaxed S_1 state of **8** can be characterized as a σ*(S–S)→σ*(S–O) excitation. Thus, the molecule excited to the S_1 state is expected to be easily converted to the dissociation products. Knowledge of the details of the excited-state reaction pathway is needed for further discussion. It should be noted, however, that the stabilization energies due to the structural relaxation on the S_1 potential energy surface were calculated to be relatively large, 17.6 (STO-3G*) and 19.0 (3-21G(*)) kcal mol^{-1}. Therefore, the excited molecule is expected to have enough energy to surmount the barrier which must exist in the course of the conversion to the product.

Conclusion

Direct irradiation of 2-phenylnaphtho[1,8-*de*][1,3]dithiin 1-oxide (**4a**), 5-phenyl[1]benzothieno[4,3,2-*def*][1,3]benzodithiepin 4-oxide (**4b**), and 2-phenyldibenzo[*d,f*][1,3]dithiepin 1-oxide (**4c**) with a 500W high

pressure mercury lamp at room temperature gave the corresponding disulfide, naphtho[1,8-*cd*][1,2]dithiole (**1a**), [1]benzothieno[4,3,2-*cde*][1,2]benzodithiin (**1b**), and dibenzo[*c,e*][1,2]dithiin (**1c**) and benzaldehyde (**7**), respectively. Inspection of all the present results shows that these photoreactions proceed through the mechanism outlined in Scheme 4. The primary photochemical event is cleavage of S(O)–CHPh bond in **4**. The partitions between recombination to starting material and formation of sulfenic ester **6** for the radical pair **5** should be affected by the S···S interaction. *Ab initio* calculations for **8**, a model compound of **6**, showed that the S_1 state of **6** can be characterized as a σ^*(S–S)→σ^*(S–O) excitation, thus explaining the second step in which **6** decomposes to **1** and **7**.

Experimental Section

Photolysis, quantum yield, sensitization, and intensity effect experiments were performed by irradiation with a 500 W high pressure mercury lamp equipped with a glass filter and monochromator. All photoreactions were monitored and quantified by HPLC or ^{1}H-NMR. X-ray crystallographic analysis was performed on an Enraf-Nonius CAD4 computer controlled κ axis diffractometer (23 ± 1 °C). Elemental analyses were carried out by Chemical Analysis Center at the University of Tsukuba.

Naphtho[1,8-*cd*][1,2]dithiole (**1a**),[10], dibenzo[*c,e*][1,2]dithiin (**1c**),[21] and 1,9-bis(methylthio)-dibenzothiophene[13] were prepared according to the methods reported in the literature. 1,8-Naphthalenedithiol (**2a**), 1,9-dibenzothiophenedithiol (**2b**), and 1,1'-biphenyl-2,2'-dithiol (**2c**) were prepared by the reduction of the corresponding disulfide (**1**) with $NaBH_4$ in ethanol–THF.[11]

Synthesis of [1]Benzothieno[4,3,2-*cde*][1,2]benzodithiin (1b). The procedure described by Testaferri and co-workers was modified for this preparation.[14] To a solution of 1,9-bis(methylthio)dibenzothiophene (1.4g, 5.1 mmol) in 40 mL of *N,N*-dimethylformamide was added a large excess of sodium methylthiolate (3.6 g, 51 mmol) with stirring under reflux conditions. After 3 h, the solution was quenched with a 10 ml of 10% HCl solution at room temperature and the methanethiole was trapped by iodine-ethanol solution. The mixture was extracted with ether and then iodine was added until the ether layer changed to a brown color. The ethereal solution was washed with saturated aqueous sodium thiosulfate, dried over anhydrous magnesium sulfate, and concentrated. The residue was separated by silica-gel column chromatography (eluent, hexane) and then recrystallization from hexane to yield yellow crystals of disulfide **1b** (1.2 g) in 92%.

[1]Benzothieno[4,3,2-*cde*][1,2]benzodithiin (1b)[22]: m.p.130 °C; ^{1}H-NMR (270 MHz, $CDCl_3$) δ 7.24 (d, J = 7.8 Hz, 2H), 7.37 (t, J = 7.8 Hz, 2H), 7.58 (d, J = 7.8 Hz, 2H); ^{13}C-NMR (67.8 MHz, $CDCl_3$) δ 121.7, 121.9, 128.1, 128.2, 131.8, 140.4; MS (m/z) 246 (M^+).

Synthesis of Dithioacetals 3a–c. General Procedure.[12] To a well stirred solution of 5 mmol of benzaldehyde (**7**) and 5 mmol of disulfide (**1a-c**) in 20 mL of CH_2Cl_2 at –20 °C was added dropwise 5 mmol of tetrachlorosilane. The solution was warmed to room temperature and monitored by TLC. When the reaction was completed (within 2 h), the solution was quenched with a 10 mL of 5% sodium bicarbonate solution and extracted with CH_2Cl_2 (3 × 100 mL). After drying with magnesium sulfate and removal of the solvent, the residue was separated by silica-gel column chromatography (eluent, tetrachloromethane) and then recrystallization from ethyl acetate–hexane gave the pure product.

2-Phenylnaphtho[1,8-*de*][1,3]dithiin (3a): Yield 98%; m.p. 124–125 °C; ^{1}H-NMR (270 MHz, $CDCl_3$) δ 5.42 (s, 1H), 7.36–7.49 (m, 7H), 7.55–7.58 (m, 2H), 7.70–7.73 (m, 2H); ^{13}C-NMR (67.8 MHz, $CDCl_3$) δ 46.83, 125.27, 125.48, 125.91, 127.71, 128.84, 129.02, 129.06, 132.04, 135.06, 136.51; MS (m/z) 280 (M^+); Anal. Calcd for $C_{17}H_{12}S_2$: C, 72.82, H, 4.31. Found: C, 72.71, H, 4.21.

5-Phenyl[1]benzothieno[4,3,2-*def*][1,3]benzodithiepin (3b): Yield 79%; m.p. 167-169 °C; ^{1}H-NMR (270 MHz, $CDCl_3$) δ 5.69 (s, 1H), 7.28-7.33 (m, 2H), 7.36-7.51 (m, 7H), 7.71-7.75 (m, 2H); ^{13}C-NMR (67.8 MHz, $CDCl_3$) δ 54.7, 120.9, 125.6, 126.2, 127.0, 128.7, 129.2, 132.9, 134.6, 137.6, 141.9 MS (m/z) 336 (M^+); Anal. Calcd for $C_{19}H_{12}S_3$: C, 67.82; H, 3.59. Found: C, 67.60; H, 3.45

2-Phenyldibenzo[*d,f*][1,3]dithiepin (3c): Yield 75%; m.p. 130-131 °C; ^{1}H-NMR (270 MHz, $CDCl_3$) δ 5.86 (s, 1H), 7.23-7.61 (m, 12H), 7.73 (d, J = 7.6 Hz, 1H,); ^{13}C-NMR (67.8 MHz, $CDCl_3$) δ 66.6, 127.0, 128.4, 128.57, 128.64, 129.67, 129.76, 129.99, 130.02, 130.2, 133.0, 135.3, 136.7, 141.6, 147.0, 147.5; MS, m/z 306 (M^+); Calcd for $C_{19}H_{14}S_2$: C, 74.47; H, 4.60. Found: C, 74.52; H, 4.54.

General Procedure for Dithioacetal 1-Oxides 4a–c. To a solution of dithioacetals **3a-c** (1.5 mmol) in 50 ml dichloromethane, *m*-chloroperbenzoic acid (259 mg, 1.5 mmol, purified by Furia's method[23]) dissolved in 50 ml dichloromethane was added at -20 °C. The solution was stirred for 12 h and then allowed to warm to room temperature. Ammonia gas was bubbled into the reaction mixture for a few minutes at room temperature, and a white precipitate of ammonium *m*-chlorobenzoate formed. The white solid was filtered off and the solvent was evaporated. The reaction mixture was purified by silica-gel column chromatograpy (eluent, ethyl acetate-hexane) to give the products as a mixture of the diasteroisomers.

2-Phenylnaphtho[1,8-*de*][1,3]dithiin 1-oxide: 4a; Yield 80%; m.p. 150-151 °C; ^{1}H-NMR (270 MHz, $CDCl_3$) δ 4.92 (s, 1H), 7.45-7.59 (m, 6H), 7.62 (dd, J_1 = 7.6 Hz, J_2 = 1.4 Hz, 1H), 7.72 (t, J = 7.6 Hz, 1H), 7.84 (dd, J_1 = 7.6 Hz, J_2 = 1.4 Hz, 1H), 8.30 (dd, J_1 = 7.6 Hz, J_2 = 1.4 Hz, 1H), 8.28 (dd, J_1 = 7.6 Hz, J_2 = 1.4 Hz, 1H); ^{13}C-NMR (67.8 MHz, $CDCl_3$) δ 63.45, 125.93, 126.16, 126.22, 126.33, 126.78, 127.48, 128.91, 129.13, 129.31, 129.65, 131.70, 131.73, 134.34, 141.60; IR (KBr) 1054 cm^{-1} (SO); MS (m/z) 296 (M^+); Anal. Calcd for

$C_{17}H_{12}OS_2$: C, 68.89, H, 4.08. Found: C, 68.74, H, 3.97. **4a'**; Yield 16%; mp. 137-138 °C; ^{1}H-NMR (270 MHz, $CDCl_3$) δ 5.35 (s, 1H), 7.45-7.59 (m, 5H), 7.71 (t, J = 7.6 Hz, 1H), 7.76 (t, J = 7.6 Hz, 1H), 7.89 (dd, J_1 = 7.6 Hz, J_2 = 1.4 Hz, 1H), 7.98 (dd, J_1 = 7.6 Hz, J_2 = 1.4 Hz, 1H), 8.12 (dd, J_1 = 7.6 Hz, J_2 = 1.4 Hz, 1H), 8.20 (dd, J_1 = 7.6 Hz, J_2 = 1.4 Hz, 1H); ^{13}C-NMR (67.8 MHz, $CDCl_3$) Broad peaks; IR (KBr) 1036 cm^{-1} (SO); MS (m/z) 296 (M^+); Anal. Calcd for $C_{17}H_{12}OS_2$: C, 68.89, H, 4.08. Found: C, 68.83, H, 4.10.

5-Phenyl[1]benzothieno[4,3,2-*def*][1,3]benzodithiepin 4-oxide: 4b; Yield 56%; m.p. 169-171 °C; ^{1}H-NMR (270 MHz, $CDCl_3$) δ 5.63 (s, 1H), 7.28-7.30 (m, 3H), 7.36-7.40 (m, 2H), 7.44 (t, J = 7.8 Hz, 1H), 7.56 (t, J = 7.8 Hz, 1H), 7.66 (d, J = 7.8 Hz, 1H), 7.78 (d, J = 7.8Hz, 1H), 7.95 (d, J = 7.8 Hz, 1H), 8.00 (d, J = 7.8 Hz, 1H); ^{13}C-NMR (67.8 MHz, $CDCl_3$) δ 66.9, 120.5, 124.8, 125.8, 126.3, 126.6, 127.4, 127.5, 128.9, 129.0, 130.0, 131.2, 133.6, 134.3, 139.1, 141.5, 142.5; MS (m/z) 352 (M^+); IR (KBr) 1044 cm^{-1} (SO); Anal. Calcd for $C_{19}H_{12}OS_3$: C, 64.74; H, 3.43. Found: C, 64.75; H, 3.32. **4b'**; Yield 28%; m.p. 224-226 °C; ^{1}H-NMR (270 MHz, $CDCl_3$) δ 5.22 (s, 1H), 7.40-7.49 (m, 6H), 7.58 (d, J = 7.9Hz, 1H), 7.72 (t, J = 7.9Hz, 1H), 7.84 (d, J = 7.9Hz, 1H), 8.04 (d, J = 7.9Hz, 1H), 8.33 (d, J = 7.9Hz, 1H); ^{13}C-NMR (67.8 MHz, $CDCl_3$) δ 65.0, 122.2, 125.5, 125.7, 126.3, 126.9, 127.1, 128.4, 129.3, 129.7, 130.2, 132.8, 132.9, 141.3, 142.3, 142.9; MS (m/z) 352 (M^+); IR (KBr) 1044 cm^{-1} (SO); Anal. Calcd for $C_{19}H_{12}OS_3$: C, 64.74; H, 3.43. Found: C, 64.63; H, 3.33.

2-Phenyldibenzo[*d,f*][1,3]dithiepin 1-Oxide: 4c; Yield 82%; ^{1}H-NMR (270 MHz, $CDCl_3$) δ 4.97 (s, 1H), 7.41-7.64 (m, 9H), 7.65-7.74 (m, 2H), 7.85-7.89 (m, 1H), 8.15-8.18 (m, 1H); ^{13}C-NMR (67.8 MHz, $CDCl_3$) δ 76.5, 122.5, 128.1, 128.4, 128.9, 129.0, 129.2, 129.4, 129.7, 130.6, 130.8, 131.3, 135.9, 138.2, 138.9, 141.4, 144.3; MS, m/z 322 (M^+); IR (KBr) 1044, 1067 cm^{-1} (SO); Anal. Calcd for $C_{19}H_{14}OS_2$: C, 70.77; H, 4.38. Found: C, 70.64; H, 4.16. **4c'**; Yield 8%; ^{1}H-NMR (270 MHz, $CDCl_3$) δ 6.09 (s, 1H, CH), 7.11 (d, J = 7.6 Hz, 2H), 7.23 (d, J = 7.6 Hz, 1H), 7.34 (t, J = 7.6 Hz, 2H, ArH), 7.39-7.48 (m, 4H), 7.50 (t, J = 7.6 Hz, 1H), 7.58(d, J = 7.6 Hz, 1H), 7.68 (d, J = 7.6Hz, 1H), 7.83 (d, J = 7.6 Hz, 1H); ^{13}C-NMR (67.8 MHz, $CDCl_3$) δ 73.3, 125.2, 127.7, 127.9, 128.0, 128.1, 128.5, 129.5, 129.7, 129.8, 130.6, 130.9, 131.3,136.0, 137.1, 139.3, 144.3; MS, m/z 322 (M^+); IR (KBr) 1044, 1069 cm^{-1} (SO); Anal. Calcd for $C_{19}H_{14}OS_2$: C, 70.77; H, 4.38. Found: C, 70.70; H, 4.22.

General Photolysis Procedure. A solution of sulfoxides **4a-c** (1 mmol) in solvent (20 mL) was placed in a Pyrex round-bottomed flask equipped with a stirrer bar and a silicon septum. The solution was bubbled with Ar for 30 min to remove O_2. Irradiation of the sample was carried out using the output of a 500 W high pressure mercury lamp filtered through a Toshiba UVD33S filter under conditions of complete light absorption. The reaction progress was monitored by HPLC or ^{1}H-NMR spectroscopy. After irradiation, the products were identified on the basis of a comparison of the respective GC, GC-mass, HPLC, and/or ^{1}H-NMR data of the authentic samples.

Irradiation of Sulfoxides 4a-c at 313 nm. A solution of sulfoxides **4a-c** (0.5 mmol) in CH_2Cl_2 (10 ml) was placed in a cylindrical quartz tube equipped with a stirring bar and a silicon septum. The solution was bubbled with Ar for 30 min to remove O_2. Irradiation of samples was carried out using the output of a 500 W high pressure mercury lamp filtered through a Toshiba UVD33S filter and a monochromator set at 313 nm under conditions of complete light absorption. The reaction progress was monitored by HPLC. After irradiation, the solvent was evaporated. Sulfenic esters **6a** and **6b** were unable to be isolated by silica-gel chromatography which results in decomposition of **6a** and **6b,** and hence the compounds **6a** and **6b** were obtained by preparative HPLC. Compounds **6a** and **6b** were approximately 95 and 89% pure, respectively, as determined by ^{1}H-NMR spectroscopy. The major impurities were **1a**, **1b** and **7**, respectively. The sulfenic ester **6c** could not be obtained from the reaction mixture by preparative HPLC.

3-Hydro-3-phenylnaphtho[1,8-*ef*][1,4]dithia[2]oxepine (6a): Oil; ^{1}H-NMR (400 MHz, $CDCl_3$) δ 6.73 (s, 1H), 7.29-7.35 (m, 5H), 7.36-7.42 (m, 2H), 7.63-7.68 (m, 2H), 7.79-7.82 (m, 2H); ^{13}C-NMR (100 MHz, $CDCl_3$) δ 97.17, 125.73, 126.14, 126.25, 128.49, 128.82, 128.90, 130.92, 131.24, 131.38, 134.35, 134.62, 136.48, 138.44, 139.08; MS (m/z) 296 (M^+).

5-Hydro-5-phenyl[1]benzothueno[4,3,2-*efg*][1,4]benzodithio[2]oxocin (6b): ^{1}H-NMR (270 MHz, $CDCl_3$, 55 °C) δ 6.38 (bs, 1H), 7.22-7.41 (m, 8H), 7.67 (d, J = 8.7 Hz, 1H), 7.69 (d, J = 8.7 Hz, 1H), 7.78 (d, J = 8.7 Hz, 1H); MS (m/z) 352 (M^+).

Quantum Yields. The measurement of the quantum yield was carried out in a cylindrical quartz tube equipped with a stirring bar and a silicon septum using the output of a 500 W high pressure mercury lamp filtered through a Toshiba UVD33S filter and a monochromator set at 313 nm under conditions of complete light absorption. The fulgide, (*E*)-α-(2,5-dimethyl-3-furyl-ethylidene)(isopropylidene)succinic anhydride, which has a quantum yield of 0.20 for its photocolouration at 313 nm in toluene was used as an actinometer.[15] Quantification was performed with HPLC. Maleic anhydride was used as an external standard for HPLC. Sample and actinometer cells were sequentially irradiated. The actinometer cells were used to determine the photo flux, which was then used to convert the rate of loss of the material into a quantum yield. Quantum yield was determined from the solution that began at the concentration of 6 mM, and conversions were kept under 5%. The measurement of the quantum yields was repeated several times by HPLC detection.

Effect of Light Intensity. The measurement of the light intensity effect was carried out using a cylindrical quartz tube equipped with a stirring bar and a silicon septum using the output of a 500 W high pressure mercury lamp filtered through a Toshiba UVD33S filter and a monochromator set at 313 nm under conditions of complete light absorption. The light intensity was attenuated by using a quartz filter (313 nm;

27, 52, and 83%). Quantification was done with HPLC. Maleic anhydride was used as an external standard for HPLC. Yields were determined from the solutions that began at the concentration of 6 mM, and irradiation times were kept under 1 h. The measurement of yields was repeated several times by HPLC detection.

X-ray Analysis of 4b. X-ray diffraction analysis on **4b** was carried out on an Enraf-Nonius CAD4 computer controlled κ axis diffractometer. The structure of **4b**, $C_{19}H_{12}OS_3$ (F.W. 352.48), was determined from the data of a crystal of dimension 0.4 × 0.4 × 0.2 mm. The space group was found to be $P2_1/n$ with unit cell a = 14.846(2) Å, b = 5.1048(6) Å, c = 20.73(2) Å, β = 95.21(2)°, V = 1564.3(8) Å^3, z = 4, ρ = 1.50 g/cm^3, μ = 4.74 cm^{-1}, F(000) = 728. The cell dimensions were determined from the setting angles of 25 reflections with $10 < \theta < 21°$ using Mo Kα radiation (λ = 0.71073 Å). A total of 3196 reflections were measured ($2\theta < 50°$) using the $\omega - 2\theta$ step scan technique. All data processing was performed on an Indy workstation by using the teXsan crystallographic software package from Molecular Structure Corp. An empirical absorption correction based on series of ψ scans was also applied to the data. The structure was refined by full-matrix least-squares where the function minimized was $\Sigma\omega(|Fo| - |Fc|)^2$, and the weight ω is defined as 1.0 for all observed reflections. All hydrogen atoms were located, and their positions were refined during the least-squares calculations; but, their isotropic thermal parameters were fixed. The final R and R_w values converged at 0.042 and 0.041, respectively. Tables of fractional atomic coordinates, thermal parameters, bond lengths and angles have been deposited at the Cambridge Crystallographic Data Center, 12 Union Road, Cambridge CB2 1EZ, United Kingdom.

X-ray Analysis of 4c. X-ray diffraction analysis on **4c** was carried out on an Enraf-Nonius CAD4 computer controlled κ axis diffractometer. The structure of **4c**, $C_{38}H_{28}S_4O_{2.50}$ (F.W. 650.86), was determined from the reflection data of a monoclinic crystal of dimension 0.4 × 0.6 × 0.6 mm. The space group was found to be $P2_1/n$ with unit cell a = 17.569(4) Å, b = 9.627(3) Å, c = 19.955(5) Å, β = 110.64(2)°, V = 3158(1) Å^3, z = 4, ρ = 1.369 g/cm^3, μ = 3.37 cm^{-1}, F(000) = 1352. The cell dimensions were determined from the setting angles of 25 reflections with $15 < \theta < 22°$ using Mo Kα radiation (λ = 0.71073 Å). A total of 6077 reflections were measured ($2\theta < 49.9°$) using the $\omega - 2\theta$ step scan technique. All data processing was performed on an Indy workstation by using the teXsan crystallographic software package from Molecular Structure Corp. An empirical absorption correction based on series of ψ scans was also applied to the data. The structure was refined by full-matrix least-squares where the function minimized was $\Sigma\omega(|Fo| - |Fc|)^2$, and the weight ω is defined as 1.0 for all observed reflections. All hydrogen atoms were located, and their positions were refined during the least-squares calculations; but, their isotropic thermal parameters were fixed. The final R and R_w values converged at 0.065 and 0.056, respectively. Tables of fractional atomic

coordinates, thermal parameters, bond lengths and angles have been deposited at the Cambridge Crystallographic Data Center, 12 Union Road, Cambridge CB2 1EZ, United Kingdom.

Acknowledgment

This work was supported by a special grant from University of Tsukuba [**TARA** project].

References

1. Martin, H.-D.; Mayer, B. *Angew. Chem., Int. Ed. Engl.* **1983**, *22*, 283.
2. Setzer, W. N.; Coleman, B. R.; Wilson, G. S.; Glass, R. S. *Tetrahedron* **1981**, *37*, 2743.
3. Glass, R. S.; Andruski, S. W.; Broeker, J. L.; Firouzabadi, H.; Steffen, L. K.; Wilson, G. S. *J. Am. Chem. Soc.* **1989**, *111*, 4036.
4. (a) Musker, W. K. *Acc. Chem. Res.* **1980**, *13*, 200. (b) Asmus, K.-D. *Acc. Chem. Res.* **1979**, *12*, 436. (c) Fujihara, H.; Akaishi, R.; Furukawa, N. *J. Chem. Soc., Chem. Commun.* **1987**, 930–931. Fujihara, H.; Furukawa, N. *J. Mol. Struct. (Theochem)* **1989**, *186*, 261. (d) Fujihara, H.; Akaishi, R.; Erata, T.; Furukawa, N. *J. Chem. Soc., Chem. Commun.* **1989**, 1789. Fujihara, H.; Akaishi, R.; Furukawa, N. *Tetrahedron* **1993**, *49*, 1605. (e) Fujihara, H.; Ninoi, T.; Akaishi, R.; Erata, T.; Furukawa, N. *Tetrahedron Lett.* **1991**, *32*, 4537. Fujihara, H.; Ishitani, H.; Takaguchi, Y.; Furukawa, N. *Chem. Lett.* **1995**, *571*. Takaguchi, Y.; Fujihara, H.; Furukawa, N. *Organometallics* **1996**, *15*, 1913. (f) Fujihara, H.; Chiu, J.-J.; Furukawa, N. *Chem. Lett.* **1990**, 2217. (g) Glass, R. S.; Broeker, J. L.; Firouzabadi, H. *J. Org. Chem.* **1990**, *55*, 5739. (h) Glass, R. S.; Adamowicz, L.; Broeker, J. L. *J. Am. Chem. Soc.* **1991** *113*, 1067 (i) Fujihara, H.; Yabe, M.; Chiu, J.-J.; Furukawa, N. *Tetrahedron Lett.* **1991**, *32*, 4345. (j) Fujihara, H.; Nakahodo, T.; Furukawa, N. *Tetrahedron Lett.* **1995**, *36*, 6275.
5. (a) Kimura, T.; Horie, Y.; Ogawa, S.; Fujihara, H.; Iwasaki, F.; Furukawa, N. *Heterocycles* **1992**, *33*, 101. (b) Furukawa, N.; Kimura, T.; Horie, Y.; Ogawa, S.; Fujihara, H. *Tetrahedron Lett.* **1992**, *33*, 1489. (c) Kimura, T.; Horie, Y.; Ogawa, S.; Furukawa, N. *Heteroatom Chem.* **1993**, *4*, 243. (d) Kimura, T.; Ishikawa, Y.; Minoshima, Y.; Furukawa, N. *Heterocycles*, **1994**, *37*, 541. (e) Kimura, T.; Ishikawa, Y.; Ueki, K.; Horie, Y.; Furukawa, N. *J. Org. Chem.* **1994**, *59*, 7117. (f) Fujii, T.; Kusanagi, H.; Furukawa, N. *Chem. Lett.* **1996**, 655.
6. Fujihara, H.; Yabe, M.; Furukawa, N. *J. Org. Chem.* **1993**, *58*, 5291.
7. (a) Furukawa, N.; Fujii, T.; Kimura, T.; Fujihara, H. *Chem. Lett.* **1994**, 1007. (b) Fujii, T.; Kimura, T.; Furukawa, N. *Tetrahedron Lett.* **1995**, *36*, 1075. (c) Fujii, T.; Horn, E.; Furukawa, N. *Heteroatom Chem.* **1998**, *9*, 29. (d) Fujii, T.; Kimura, T.; Furukawa, N. *Tetrahedron Lett.* **1995**, *36*, 4813. (e) Fujii, T.; Sakuragi, H.; Furukawa, N. *Tetrahedron Lett.* **1995**, *36*, 8039. (f) Fujii, T.; Takahashi, O.; Furukawa, N. *J. Org. Chem.* **1996**, *61*, 6233.
8. Fujihara, H.; Chiu, J.-J.; Furukawa, N. *J. Am. Chem. Soc.* **1988**, *110*, 1280. Fujihara, H.; Mima, H.; Erata, T.; Furukawa, N. *J. Am. Chem. Soc.* **1992**, *114*, 3117. Fujihara, H.; Mima, H.; Furukawa, N. *J. Am. Chem. Soc.* **1995**, *117*, 10153. Fujihara, H.; Nakahodo, T.; Furukawa, N. *Chem. Commun.* **1996**, 311. Bergholdt, A. B.; Kobayashi, K.; Horn. E.; Takahashi, O.; Sata, S.; Furukawa, N.; Yokoyama, M.; Yamaguchi, K. *J. Am. Chem. Soc.* **1998**, *120*, 1230.
9. House, H. O.; Koepsell, D. G.; Campbell, W. J. *J. Org. Chem.* **1972**, *37*, 1003.
10. Zweig, A.; Hoffman, A. K. *J. Org. Chem.* **1965**, *30*, 3997.
11. Yui, K.; Aso, Y.; Otubo, T.; Ogura, F. *Bull. Chem. Soc. Jpn.* **1988**, *61*, 953.
12. Ku, B.; Oh, D.-Y. *Synth. Commun.* **1989**, *19*, 433.
13. Furukawa, N.; Kimura, T.; Horie, Y.; Ogawa, S. *Heterocycles* **1991**, *32*, 675.
14. Testaferri, L.; Tingoli, M.; Tiecco, M. *Tetrahedron Lett.* **1980**, *21*, 3099.
15. Heller, H. G.; Langan, J. R. *J. Chem. Soc., Perkin Trans. 2* **1981**, 341.

16. SPARTAN, Version 3.1: Wavefunction, Inc., Irvine, CA.
17. GAUSSIAN 92, Revision G.4: Frisch, M. J.; Trucks, G. W.; Head-Gordon, M.; Gill, P. M. W.; Wong, M. W.; Foresman, J. B.; Johnson, B. G.; Schlegel, H. B.; Robb, M. A.; Replogle, E. S.; Gomperts, R.; Andres, J. L.; Raghavachari, K.; Binkley, J. S.; Gonzalez, C.; Martin, R. L.; Fox, D. J.; Defrees, D. J.; Baker, J.; Stewart, J. J. P.; Pople, J. A. Gaussian, Inc., Pittsburgh, PA (1992).
18. (a) Still, I. W. J. in "The chemistry of sulphones and sulphoxides," ed by Patai, S.; Rappoport, Z.; Stirling, C. J. M.; John Wiley & Sons Ltd., Chichester (1988), p. 873 and references therein. (b) Schultz, A. G.; Schlessinger, R. H. *J. Chem. Soc., Chem. Commun.*, **1970**, 1294. (c) Guo, Y.; Jenks, W. S. *J. Org. Chem.*, **1995**, *60*, 5480. (d) Guo, Y.; Jenks, W. S. *J. Org. Chem.*, **1997**, *62* 857.
19. Kowalewski, R.; Margaretha, P. *Helv. Chim. Acta* **1993**, *76*, 1251. (b) Capps, N. K.; Davies, G. M.; Hitchcock, P. B.; McCabe, R. W.; Young, D. W. *J. Chem. Soc., Chem. Commun.* **1983**, 199.
20. Pasto, D. J.; L'Hermine. G. *J. Org. Chem.*, **1990**, *55*, 5815.
21. Murata, S.; Suzuki, T.; Yanagisawa, A.; Suga, S. *J. Heterocyclic Chem.* **1991**, *28*, 433.
22. Cossu, S.; De Lucchi, O.; Piga, E.; Valle, G. *Phosphrous, Sulfur, and Silicon* **1991**, *63*, 55.
23. Bortolini, O.; Campestrini, S.; Di Furia, F.; Modena, G. *J. Org. Chem.* **1987**, *52*, 5093.